

## Supporting Information

# New ICT-based ratiometric two-photon near infrared probe for imaging tyrosinase in living cells, tissues and whole organisms.

Javier Valverde-Pozo<sup>1</sup>, Jose Manuel Paredes<sup>1,\*</sup>, M. Eugenia Garcia-Rubiño<sup>1</sup>, Thomas J. Widmann<sup>2</sup>, Carmen Griñan-Lison<sup>2, 3, 4</sup>, Silvia Lobon-Moles<sup>1</sup>, Juan A. Marchal<sup>3, 5, 6</sup>, Jose M. Alvarez-Pez<sup>1</sup> and Eva M. Talavera<sup>1,\*</sup>

<sup>1</sup> Nanoscopy-UGR Laboratory, Department of Physical Chemistry, Faculty of Pharmacy, Unidad de Excelencia en Química Aplicada a Biomedicina y Medioambiente (UEQ), University of Granada, C. U. Cartuja, 18071 Granada, Spain.

<sup>2</sup> GENYO, Centre for Genomics and Oncological Research, Pfizer/University of Granada/Andalusian Regional Government, 18016 Granada, Spain.

<sup>3</sup> Instituto de Investigación Biosanitaria (ibs.GRANADA), 18012 Granada, Spain.

<sup>4</sup> UGC de Oncología Médica, Complejo Hospitalario de Jaen, 23007 Jaen, Spain.

<sup>5</sup> Centre for Biomedical Research (CIBM), Biopathology and Regenerative Medicine Institute (IBIMER), University of Granada, 18100 Granada, Spain.

<sup>6</sup> Department of Human Anatomy and Embryology, Faculty of Medicine, University of Granada, 18016 Granada, Spain.

\* Correspondence: etalaver@ugr.es; Tel.: +34 958243828 (optional; include country code; if there are multiple corresponding authors, add author initials); [jmparedes@ugr.es](mailto:jmparedes@ugr.es); Tel.: +34 958243829

## Index

Figure S1. Synthesis of compound DCM-HBU.	2
Mass and NMR spectra.	3
Figure S2. Absorption spectra of the DCM-HBU at different concentrations.	4
Figure S3. Molar absorptivity coefficient calculation.	4
Figure S4. Emission spectra of the DCM-HBU at different concentrations.	5
Quantum yield calculation.	5
Figure S5. Fluorescence decays of DCM-NH <sub>2</sub> and DCM-HBU.	6
Figure S6. Evolution of the emission spectra of DCM-HBU with TYR.	7
Figure S7. Influence of pH and temperature on enzyme activity.	7
Figure S8. IR spectra.	8
Figure S9. Representative images of the green and red intensity channels and R:G ratio images of A-375 and MEL1 cells after adding DCM-HBU.	9
Figure S10. Increase in the value of the ratio versus time of the images of MEL1 and A-375 cells.	9
Figure S11. Representative images of the green and red intensity channels of A-375 tumours after adding DCM-HBU using two-photon microscopy.	10
Figure S12. 3D red and green intensity images of A-375 tumours after adding DCM-HBU using two-photon microscopy.	10
Figure S13. Top and bottom planes of 3D ratiometric images of A-375 tumours.	11
Figure S14. Images of living zebrafish embryos and larvae incubated with DMSO.	11
Video S1. Fluorescence microscopy R:G ratio maps of live A-375 cell line after adding DCM-HBU and representation of the R:G ratio values over time, by two-photon excitation.	11
Video S2. 3D ratiometric images of A-375 tumours.	11

### Synthesis of DCM-HBU

To a solution of compound 1 (80 mg, 0.26 mmol) in dichloromethane (12.82 mL) under a N<sub>2</sub> atmosphere, triphosgene (153 µg, 5.15 × 10<sup>-4</sup> mmol) was added. The mixture was then cooled to 0-5 °C to add DIPEA (88.9 µL) and then was stirred for 3 h. Then, 4-hydroxybenzylamine (127 µg) was added and the reaction was kept at room temperature for 24 h. Then, the solvent was removed under low pressure, and the residue was submitted to flash chromatography in CH<sub>2</sub>Cl<sub>2</sub>:CH<sub>3</sub>OH mixtures to produce DCM-HBU (compound 2) as a pale-yellow solid with a 5 % yield. <sup>1</sup>H NMR (500 MHz, DMSO-*d*<sub>4</sub>) δ 8.73 (dd, *J* = 8.4, 1.3 Hz, 1H), 7.92 (ddd, *J* = 8.5, 7.2, 1.4 Hz, 1H), 7.80 (dd, *J* = 8.4, 1.1 Hz, 1H), 7.76 – 7.58 (m, 8H), 7.56 (d, *J* = 8.8 Hz, 2H), 7.32 (d, *J* = 15.9 Hz, 1H), 7.09 (dd, *J* = 8.6, 2.3 Hz, 3H), 6.98 (s, 1H), 6.72 – 6.67 (m, 3H). TOF MS ES<sup>-</sup>, calculated for C<sub>28</sub>H<sub>20</sub>N<sub>4</sub>O<sub>3</sub>Cl: 495.1224 (*M*+Cl<sup>-</sup>); found: 495.1241.

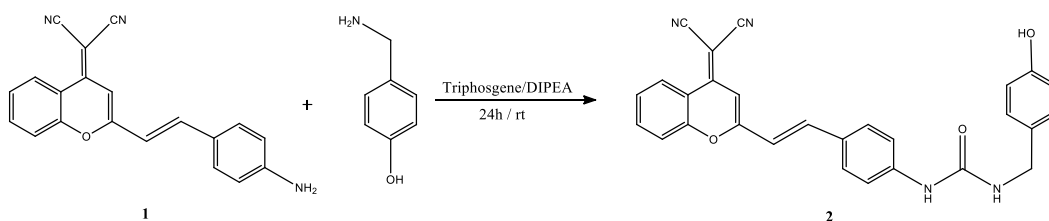


**Figure S1.** Synthesis of compound DCM-HBU.

### Mass spectrum of compound DCM-HBU

## Elemental Composition Report

Page 1

### Single Mass Analysis

Tolerance = 10.0 PPM / DBE: min = -1.5, max = 50.0

Element prediction: Off

Number of isotope peaks used for i-FIT = 3

**Monoisotopic Mass, Even Electron Ions**

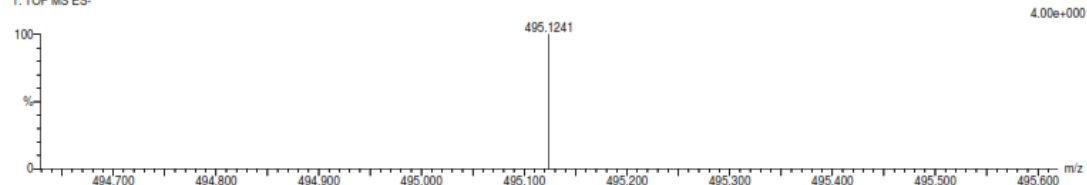
418 formula(e) evaluated with 5 results within limits (up to 50 closest results for each mass)

Elements Used:

C: 0-28 H: 0-1000 N: 0-4 O: 0-7 Na: 0-1 Cl: 0-1

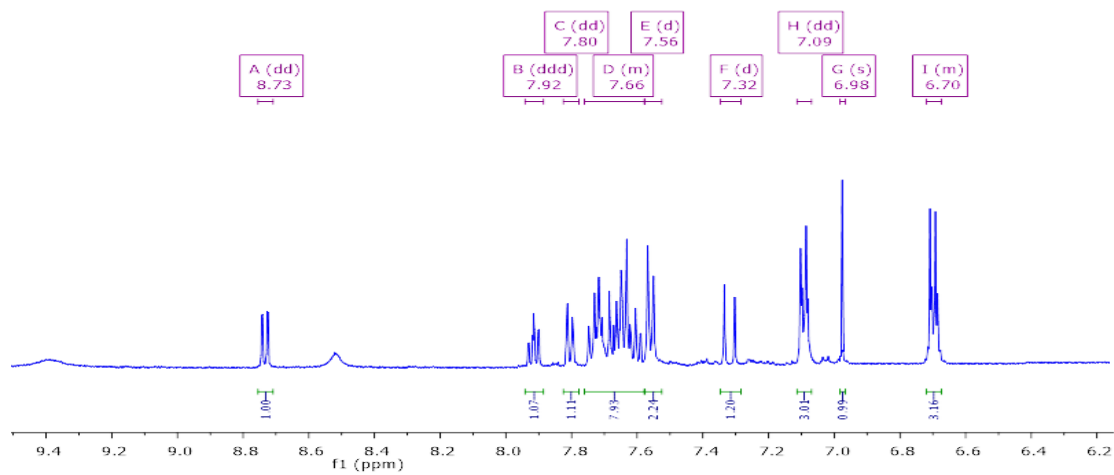
SilviaDneg 11 (0.250) AM (Top,1, Ht,5000.0,0.00,1.00)

1: TOF MS ES-



Minimum:					-1.5				
Maximum:		5.0	10.0		50.0				
Mass	Calc. Mass	mDa	PPM	DBE	i-FIT	i-FIT (Norm)	Formula		
495.1241	495.1224	1.7	3.4	20.5	12.6	1.5	C28	H20	N4 O3 C1
495.1211		3.0	6.1	15.5	12.6	1.5	C27	H24	O7 C1
495.1281		-4.0	17.5	8.1	12.8	1.7	C25	H28	N4 O6 Na
495.1200		-1.1	8.3	17.5	12.6	1.5	C26	H21	N4 O3 Na
495.1192		4.9	9.9	20.5	12.8	1.8	C28	H19	N2 O7

### <sup>1</sup>H-NMR spectrum of compound DCM-HBU



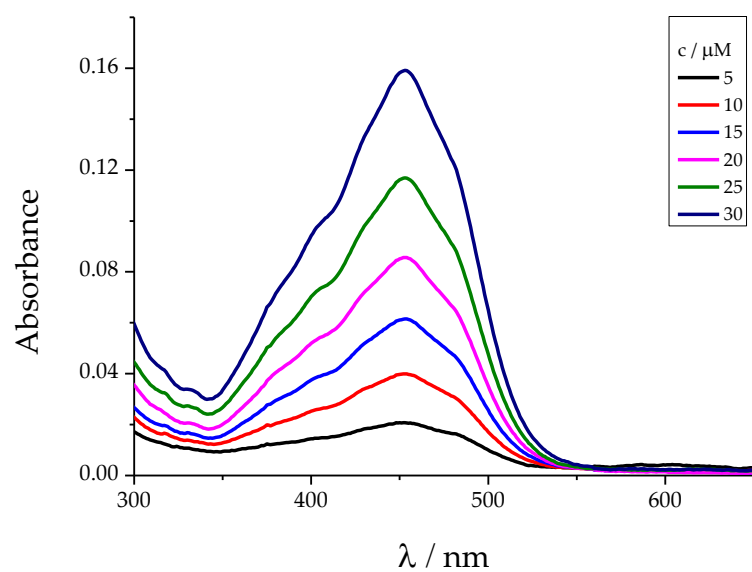


**Figure S2.** Absorption spectra of the DCM-HBU at different concentrations in PBS/DMSO (7/3, v/v).

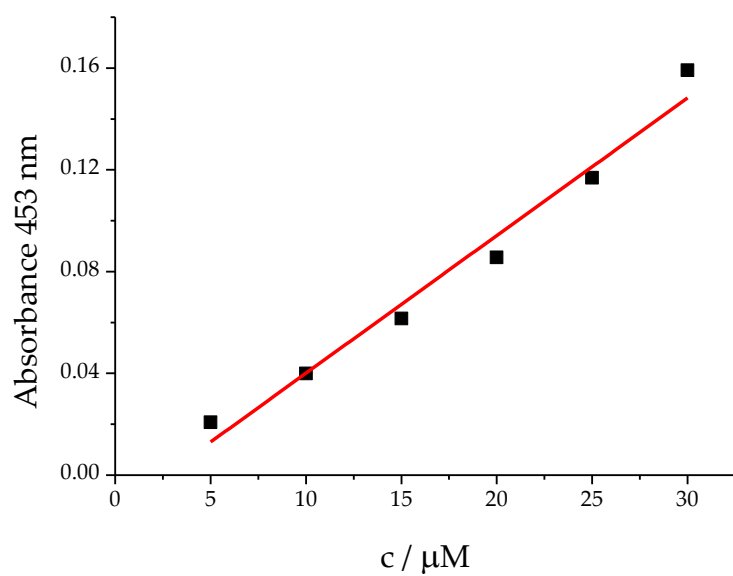


**Figure S3.** Determination of the molar absorptivity coefficient of the compound DCM-HBU in PBS /DMSO (7/3, v/v) at  $\lambda = 453$  nm. Fit equation:  $y = -0.01402 + 5.409x$ ,  $R^2 = 0.971$ .

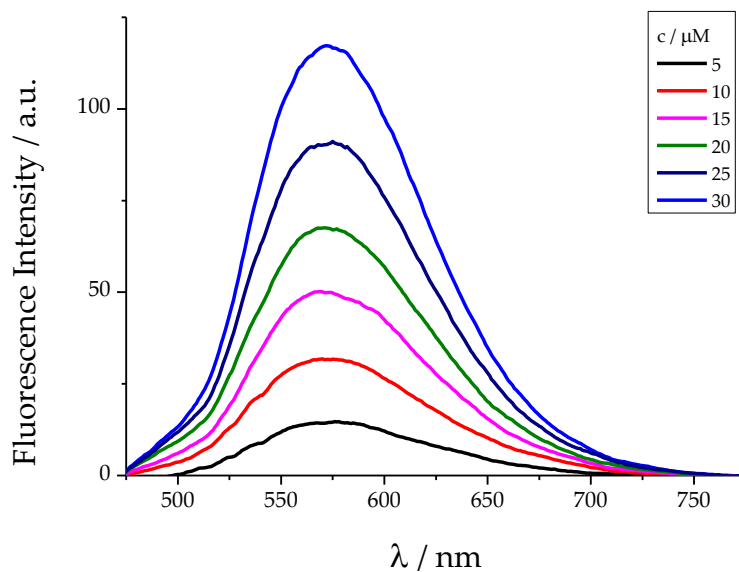


**Figure S4.** Emission spectra of the DCM-HBU at different concentrations in PBS/DMSO (7/3, v/v) by excitation at 453 nm.

#### Quantum yield calculation

The relative fluorescence quantum yield data were obtained by integrating the areas under the fluorescence curves using the expression:

$$\Phi = \Phi_R \cdot \frac{I}{I_R} \cdot \frac{OD_R}{OD} \cdot \frac{n^2}{n_R^2}$$

where  $\Phi$  and  $\Phi_R$  indicate the fluorescence quantum yields of the sample and reference, respectively;  $I$  and  $I_R$  the integrated fluorescence spectra of the sample and reference, respectively;  $OD$  and  $OD_R$  are the optical density at the excitation wavelength of the sample and reference, respectively; and  $n$  and  $n_R$  are the refractive indexes of the solvents when the sample and reference are dissolved, respectively. As references, we have used Fluorescein in NaOH 0.1M ( $\Phi = 0.91$ ) for DCM-HBU, and Rhodamine 101 in MeOH ( $\Phi = 1$ ) for DCM-NH<sub>2</sub>.

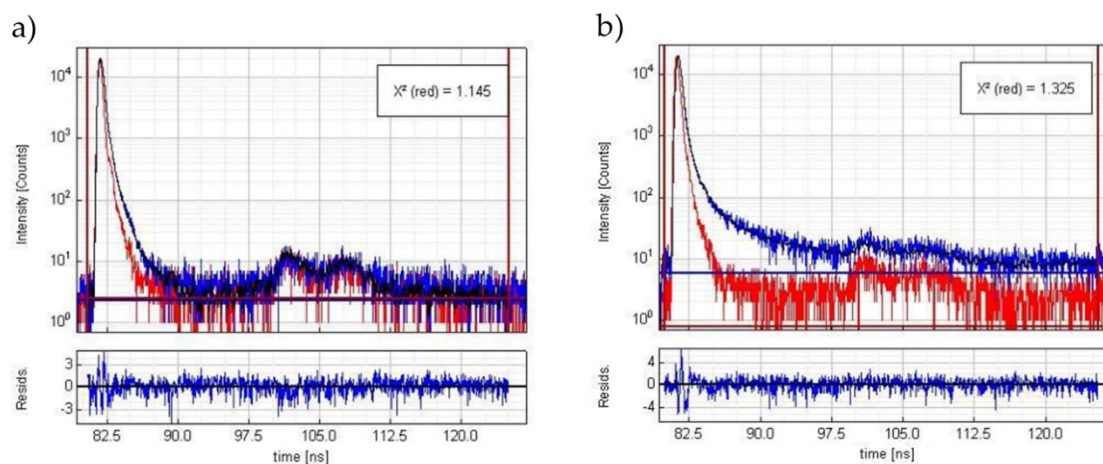


**Figure S5.** a) Fluorescence decay of DCM-NH<sub>2</sub> at  $\lambda_{\text{ex}} = 485$  nm and  $\lambda_{\text{em}} = 664$  nm. b) Fluorescence decay of DCM-HBU at  $\lambda_{\text{ex}} = 440$  nm y  $\lambda_{\text{em}} = 570$  nm.

We used the TCSPC method to register the fluorescence decay by a FluoTime 200 fluorometer (PicoQuant, Inc.). Excitation was achieved by a 485 nm or 440 nm laser-pulsed (PicoQuant, Inc.). The pulse repetition rate was 40 MHz.

Fluorescence traces were obtained in 1320 channels. The channel resolution was 36 ps. Histograms of the instrument response functions (using LUDOX scatterer) and sample decays were recorded until they reached 20 000 counts in the peak channel. Fluorescence decays were recorded at three emission wavelengths, 659, 664 and 669 nm for the sample DCM-NH<sub>2</sub> (7/3 PBS/DMSO (v/v)) and 565, 570 y 575 nm for the DCM-HBU(7/3 PBS/DMSO (v/v)).

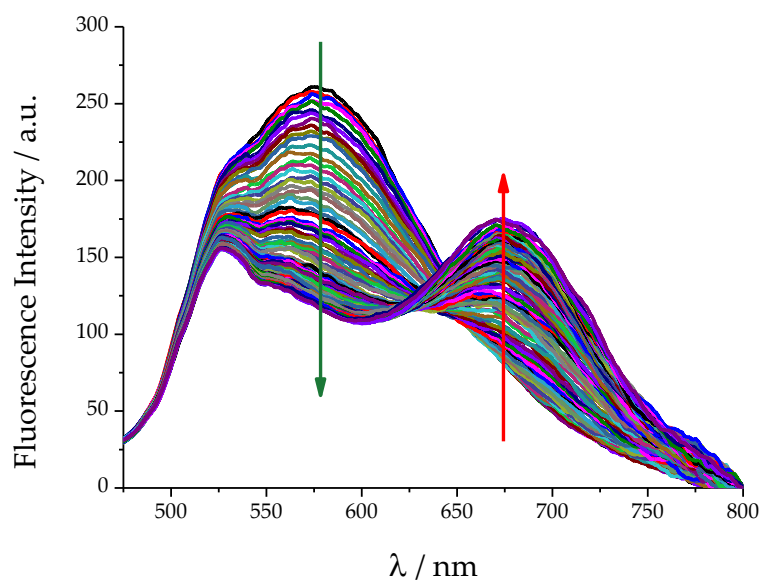


**Figure S6.** Evolution of the emission spectra of DCM-HBU (25  $\mu\text{M}$ ) with TYR (0.13  $\text{mg mL}^{-1}$ ) observed every 1 min for 2 h by excitation at 450 nm at 37  $^{\circ}\text{C}$ .

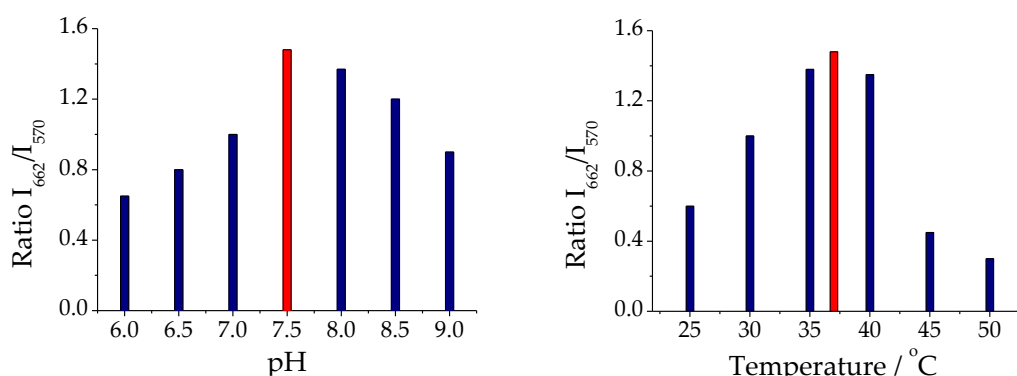


**Figure S7.** (a) Ratiometric measurements of fluorescence signals of  $I_{662}/I_{570}$  of DCM-HBU (25  $\mu\text{M}$ ) with DPP IV (0.13  $\text{mg mL}^{-1}$ ) after 2 h of incubation at 37  $^{\circ}\text{C}$  and different pHs by excitation at 450 nm. (b) Ratiometric measurements of fluorescence signals of  $I_{662}/I_{570}$  of DCM-HBU (25  $\mu\text{M}$ ) with DPP IV (0.13  $\text{mg mL}^{-1}$ ) after 2 h of incubation at different temperatures and pH 7.5  $^{\circ}\text{C}$  by excitation at 450 nm.

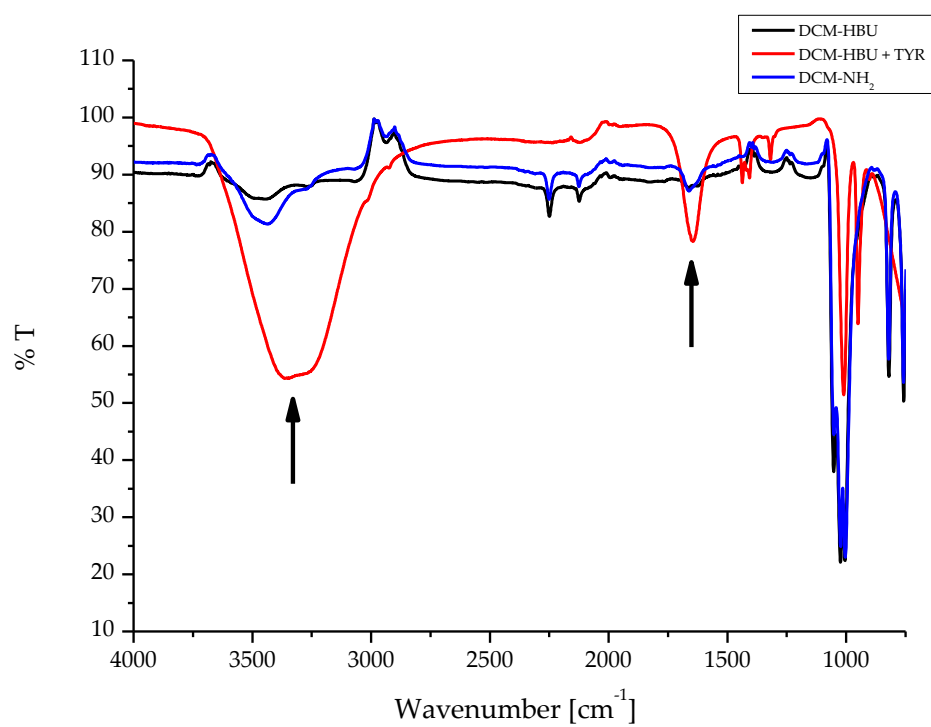


**Figure S8.** IR spectra of DCM-NH<sub>2</sub> (in DMSO), DCM-HBU (in DMSO) and DCM-HBU with TYR (in PBS/DMSO 7,3 v/v) after 2 h of reaction.



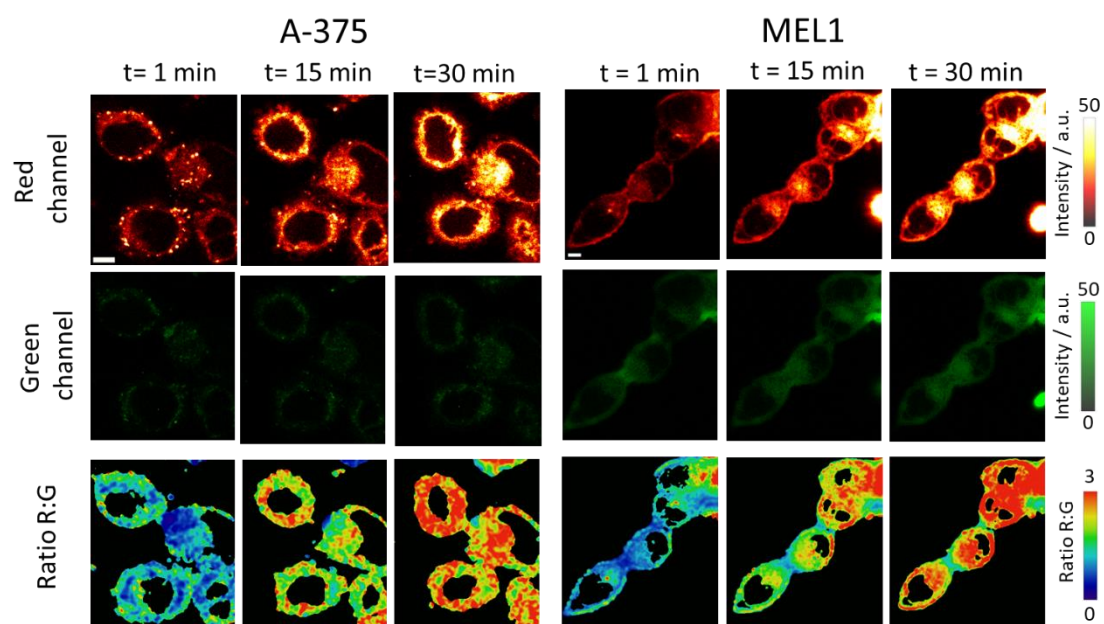


**Figure S9.** Representative images of the red ( $\lambda_{em} = 650-720$  nm) and green ( $\lambda_{em} = 502-538$  nm) intensity channels and the ratio R:G images of A-375 and MEL1 cells after adding DCM-HBU (5  $\mu$ M) over time by excitation at 453 nm. Scale bars are 5  $\mu$ m.

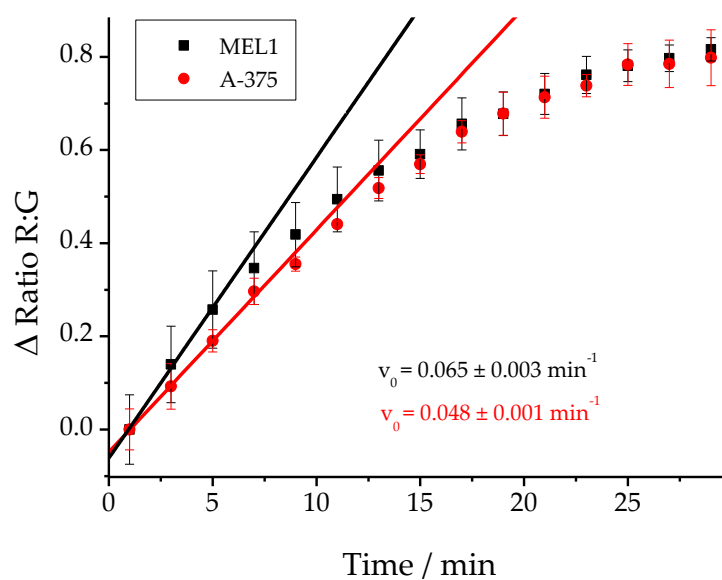


**Figure S10.** Increase in the value of the ratio versus time of the images of MEL1 and A-375 cells.

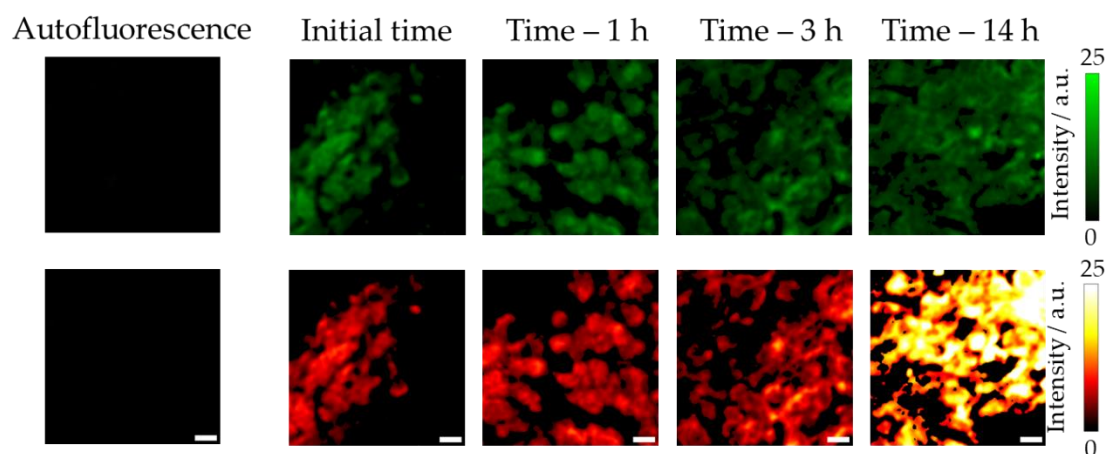


**Figure S11.** Representative images of the intensity green ( $\lambda_{em} = 502\text{-}538\text{ nm}$ ) and red ( $\lambda_{em} = 650\text{-}720\text{ nm}$ ) channels (first and second lines, respectively) of A-375 tumours after adding DCM-HBU ( $5\text{ }\mu\text{M}$ ) using two-photon microscopy with excitation at  $800\text{ nm}$ . Scale bars are  $10\text{ }\mu\text{m}$ .

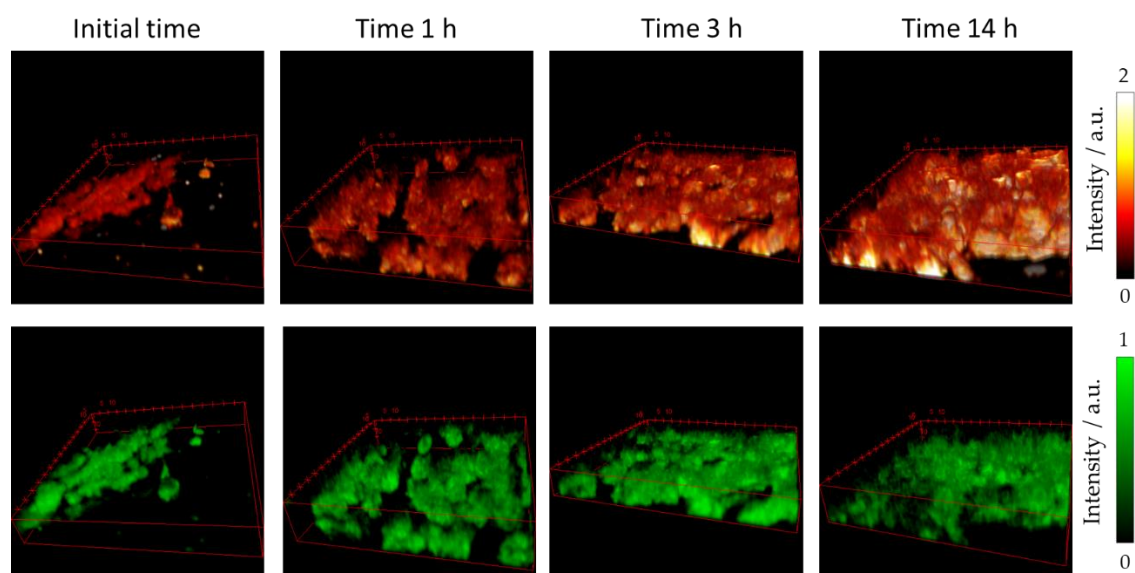


**Figure S12.** 3D red (first line) and green (second line) intensity images of A-375 tumours using two-photon microscopy with excitation at  $800\text{ nm}$

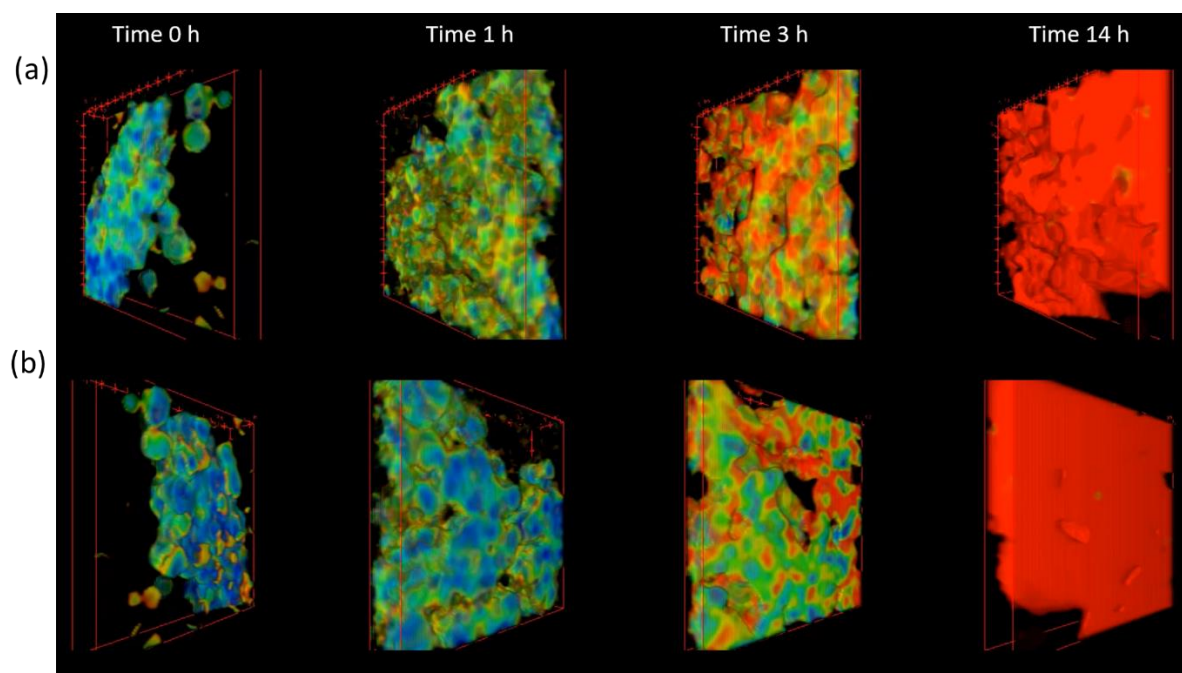


**Figure S13.** Top (a) and bottom (b) plane of 3D ratiometric images of A-375 tumours.

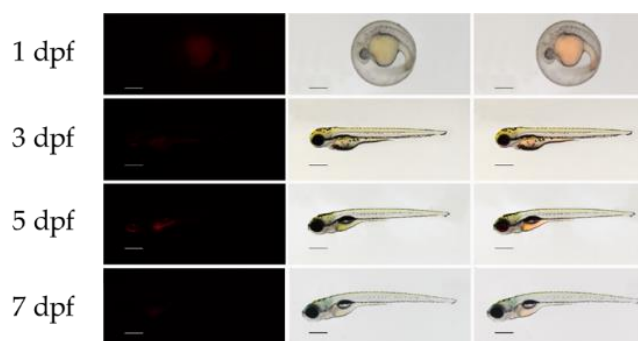


**Figure S14.** Living zebrafish embryos and larvae incubated with 10  $\mu$ M DMSO for 3 h at different days post fertilization (dpf); red fluorescent (left), brightfield (centre), and merge (right) images are taken with a stereo microscope ( $\lambda_{\text{exc}} = 458 \text{ nm}$ ;  $\lambda_{\text{em}} = 680 \text{ nm}$ ). Scale bars: 1 dpf: 250  $\mu$ m, 3-7 dpf: 500  $\mu$ m.

**Video S1.** Fluorescence microscopy R:G ratio maps of live A-375 cell line after adding DCM-HBU and representation of the R:G ratio values over time, by two-photon excitation.

**Video S2.** 3D ratiometric images of A-375 tumours.